Field Tests and Stress Analysis of Small Diameter Water Supply Pipes for Durability Evaluation

Ma Zhiliang*, Kentaro Yamada** and Tamotsu Kamiya***

* Dr. of Eng., Assoc. Professor, Dept. of Civil Eng., Tsinghua University, Beijing 100084 China
** Ph.D., Professor, Dept. of Civil Eng., Nagoya University, Furocho, Chikusa-ku, Nagoya 464-01
*** M.S., The Seiyo Corporation, Naka 9-chome, 1-2, Koyo-cho, Higashinadaka, Kobe 658

This study aims at investigating the longitudinal stress of small diameter water supply pipes for durability evaluation. New ductile iron pipes of 100 mm in diameter were buried at about 80 cm under a road. Soil pressure and strains were measured under static loading and dynamic loading by using a dump truck. Parametric analysis is carried out on the static strain in the pipes to estimate the maximum static strain and to clarify the critical influential factors. Based on the computed static strain and the test results an empirical equation is proposed to evaluate the strain of pipes for the durability evaluation.

Key Words: water supply pipe, durability, cast iron pipe

1. Introduction

Underground water supply pipes (hereafter, WSP) play an important role to support daily urban life in a modern society and are often called lifeline. They are required to provide constant service throughout their design life, which is specified as about 40 years in Japan. Since they are often installed under roads, they deteriorate for various reasons, such as internal and external corrosion and/or fatigue. If deterioration occurs, leaks and breaks take place in the pipeline. Therefore, it is necessary to develop techniques to evaluate the durability of old pipelines in order to replace them timely and effectively.

In Japan, cast iron pipes were mainly used for WSP until early 1970's. Through investigating the reasons for the breaking of WSP in Nagoya City, it was found that most breaks occurred in the small diameter pipes which constitute the majority of the total pipe length. Sampling investigation and analysis on 89 small diameter cast iron WSP were carried out and it was concluded that mere through-wall pitting can hardly cause breaks in the pipes[1]. It was also found that overloaded heavy trucks passing on the road over the pipes seemed to have caused the breaks[2]. From these facts, it was considered that the pipes may have failed mechanically due to the combined effect of the excessive stresses caused by traffic loads and the stress concentration caused by corrosion pits in the pipe wall.

The stresses in WSP may be divided mainly into three categories, i.e. initial stress introduced during installation of the pipes, stress due to temperature change and stress due to traffic load over the pipes. Among them, the maximum stress due to temperature change is estimated as 30 MPa, which is much smaller than the strength of pipe material. WSP have been designed for the stresses caused by the wheel load of trucks against the failure of pipe wall as a ring[3),4),5)]. However, small diameter WSP have mainly failed as a beam due to the longitudinal stress of pipes[2]. On the other hand, strains can be measured, and in the elastic range, the corresponding stresses can be obtained by multiplying the strain with the elastic modulus except for temperature strain, for which a conservative evaluation may be obtained depending on the constraint on the pipes. Since strain due to temperature change is relatively small in the case of WSP, this simple computation of stresses serves the purpose of durability evaluation of WSP. Therefore, the longitudinal strains in small diameter WSP are to be studied.

Field tests were carried out by Pocock et al. on new cast iron pipes of small diameter and by Takagi et al. on new ductile iron pipes, respectively[6),7)]. In the former study, local weak bedding was intentionally introduced, then the initial strains in the pipes due to installation and the strains corresponding to various rolling speed of trucks were measured. The latter study further considered the strains due to a heavy moving truck. Takagi et al. also used the theory of beams on elastic foundation in order to obtain the strain under wheel load analytically[8)]. But no systematic analysis of strain has been carried out for the purpose of durability evaluation in these studies.

In this study, new ductile iron pipes of 100 mm in diameter were buried at about 80 cm under a road, and a dump truck with the maximum weight of 253 kN was ran over the pipes at various speeds. The experimental result is

used to reconfirm the justification of the theory of beams on elastic foundation for computing the static strain of pipes and to evaluate the effect of dynamic loading. Parametric analysis is carried out on the static strain of cast iron pipes by varying factors, such as installation depth of the pipes, bedding condition, etc. to clarify the critical influential factors. Finally, an empirical equation is proposed to compute the actual strain of pipes for the durability evaluation of small diameter WSP.

2. Test Method

A part of the asphalt concrete pavement was taken off on a private road, and then a "T" shape trench of 90 cm deep and 100 cm wide was dug. Three ductile iron pipes, i.e. one parallel to the road (hereafter, pipeline I) and two across the road (hereafter, pipeline II) were installed and the part was paved again, where the two pipes in the pipeline II were connected with a mechanical joint . A double-tire dump truck with or without payload was driven on the road. The pipelines, sensors and the dimension of the truck are shown in Fig.1.

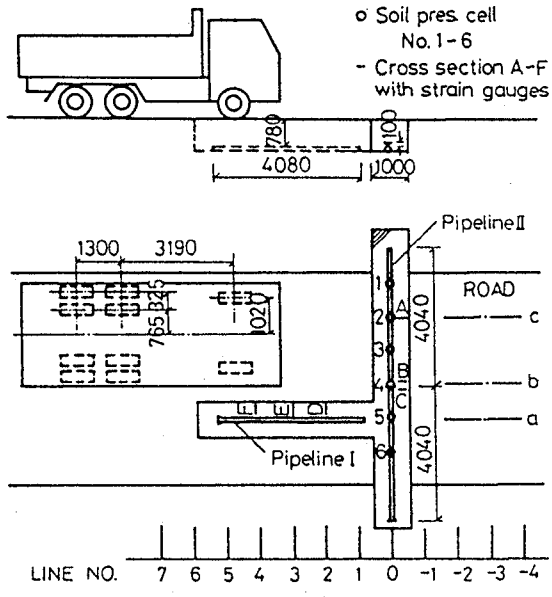

Fig.1 Test Layout (unit:mm)

All three pipes are new ductile iron pipes of 4 m in length and 100 mm in diameter with 7.5 mm thick wall and 4.0 mm thick mortar lining. Total 44 strain gauges were attached in the cross sections A to F. After the pipes were placed on the bedding layer of sand of about 10 cm thick, backfilling was carried out up to about the pipe crown using sand, and six soil pressure cells were placed at about 10 cm above the pipe crown. Two layers of sand of about 30 cm thick each were then poured into the trench and compacted manually with a wooden compactor. The rest of the backfilled sand was compacted with a compact machine. Finally, 15 cm thick gravel and 5 cm thick asphalt concrete pavement was placed. This layering of backfill is similar to the practice in Japan. The properties of the backfilled sand is shown in Table 1.

The test program is shown in Table 2. The tests were carried out five times between May 24 and Sept. 11, 1990. Both static loading and dynamic loading were conducted by using the truck, and keeping one of the front wheels running along the lines a, b or c, as shown in Fig.1. In the static loading, the strain in the pipes and the soil pressure on the pipes were measured when the truck was placed at the lines 7, 6, 5, 4, etc., as shown in Fig.1. The dynamic loading includes three modes, i.e. rolling mode, braking mode and bumping mode. In the rolling mode, the truck ran at the speed of 5, 15 and 30 km/h, respectively. In the braking mode, the truck moving at the speed of 30 km/h decelerated with brakes at 2 m before the pipes. The bumping mode simulates the condition of rough road surface, since the repair of road pavement often leaves bump-like rough surface. In the bumping mode, a bump was used as shown in Fig.2. The bump heights were adjusted to 3, 5 and 7 cm, respectively.

Table 1 Properties of the backfilled sand

soil component		grain size(mm)	percent
soil	coarse	2 to 4.76	5.0
	medium	0.42 to 2	37.3
	fine	0.074 to 0.42	33.0
silt		0.00389 to 0.0074	15.7
clay		less than 0.00389	6.3
diam. corrsp. to 10% small grain weight 0.0065 mm			
diam. corrsp. to 30% small grain weight 0.16 mm			
diam. corrsp. to 60% small grain weight 0.47 mm			
maximum diam. 19.1 uniformness coef. 72.3			
specific gravity 0.0247 N/cm^3 water content 13.2%			

Table 2 Properties of the backfilled sand

Test No.	Date	Pave Con.	Vehicle Front	Weight Rear	(kN) Total	Test Mode
1	May 24	unpaved	43.7	68.1	111.8	S.
1'	May 24	unpaved	55.1	174.6	229.7	S. R.
2	May 29	paved	61.8	174.8	236.6	S. R. BP.
3	July 26	paved	60.0	193.4	253.4	S. R. BP.
4	Sept. 11	paved	47.4	66.7	114.1	S. R. BR
5	Sept. 11	paved	55.9	192.7	248.7	S. R. BR.

Note. S : stationary, R : rolling, BP : bumping, BR : braking

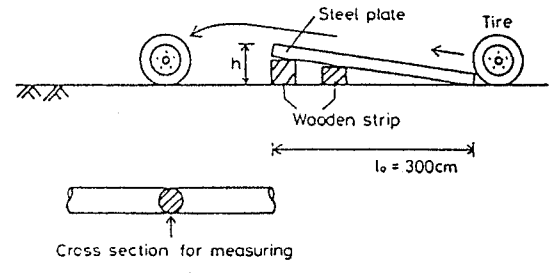

Fig.2 Bump set used in the test

A static data-logger was used to measure the static soil pressure on the pipes and the static strains in the pipes. For the dynamic loading, a set of digital dynamic data-logger was used. It made it possible to record all signals of the sensors simultaneously. In the following discussion, only the

longitudinal strains are to be presented, because the circumferential strain of the pipes was found much smaller than the longitudinal one.

3. Strains due to Static Load

3.1 Initial Strain in the Pipes

The initial strains were measured at various stages of pipe setting, and the results are shown in Fig.3. It indicates the strains at the crown and the bottom of the pipes in the cross sections A to F. The numbers 01, 02, 05, 09, 10 and 18 in the horizontal axis represent the measuring before backfilling, after the first layer of backfilling, after the second layer of backfilling, after the third layer of backfilling and just before placing pavement and after placing pavement, respectively. The maximum initial strain occurred at the cross section D was about 100 micro, which is comparable with that in Pocock's report [6].

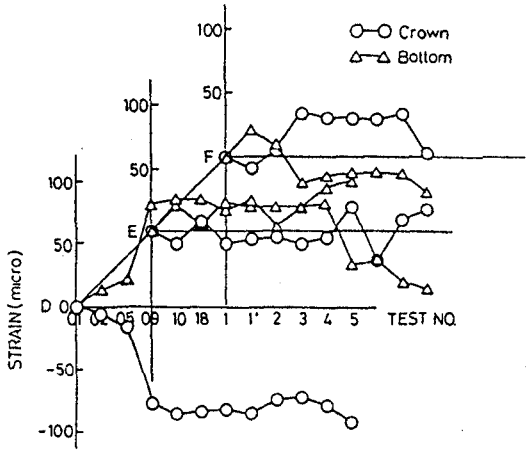

(a) for sections D, E and F of pipeline I

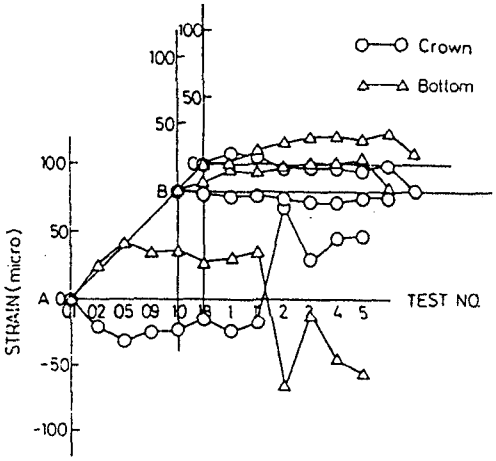

(b) for sections A, B, C of pipeline II

Fig.3 The initial strain in the pipes

3.2 Strain due to Static Wheel Loading

Static strains in the pipes were measured for a dump truck of 236 kN. The truck was placed at about 1 m interval in order to evaluate the effect of wheel position on the strains. The measured strains at the crown and the bottom of the pipes in the cross sections E and A are shown in Fig.4. It is observed that the absolute values of strains at the crown is almost equal to that at the bottom regardless of the position of the truck. It implies that the pipes are mainly subjected to bending and the strains due to axial forces are negligibly small under wheel loads.

In order to obtain the analytical result, the pipeline was modeled as connected beams on elastic foundation, as shown in Fig.5. The soil pressure due to wheel loads was computed by using Boussinesq's equation and was represented by using Fourier series. Then the stiffness matrix is computed for an beam for FEM analysis to obtain the strains in the pipeline. The reaction coefficient of bedding, k, was determined through a loading test as 22.5 N/cm^3.

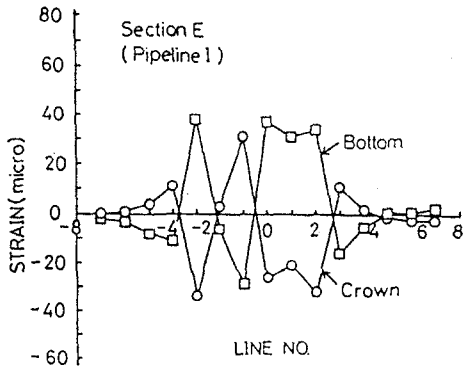

(a) for pipeline I

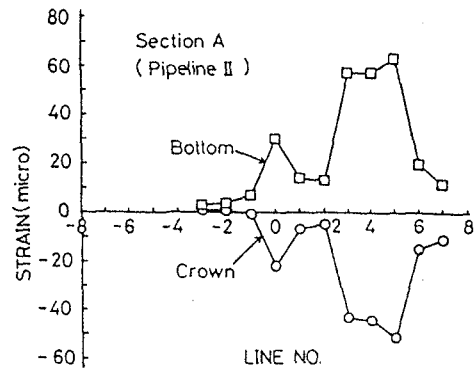

(b) for pipeline II

Fig.4 Strain in the pipes under static wheel load

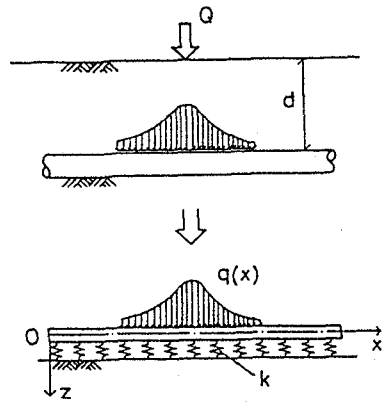

Fig.5 Analytical model of pipeline

In Fig.6, the analytical strains are compared with the measured strains in the cross section E of the pipeline I and in the cross section A of the pipeline II for various positions of the truck. It is observed that the analytical strains are in

good agreement with the measured strains.

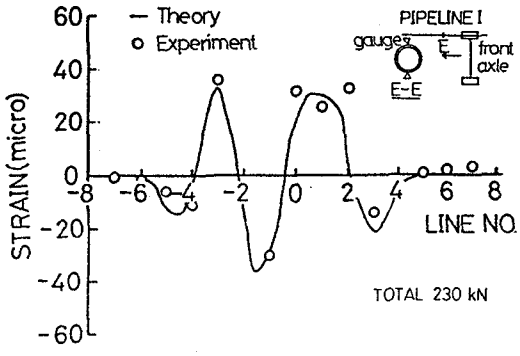

(a) The truck moves along the pipeline

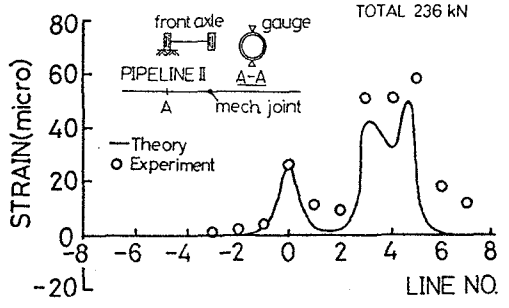

(b) The truck moves across the pipeline

Fig.6 Comparison between experimental and analytical results

4. Strains due to Dynamic Load

The strains in the section A of the pipeline I are shown in Fig.7, when the truck ran over it at the speed of 30 km/h. The effect of each wheel of the truck on the strains can easily be distinguished. As expected, larger strain is observed in both the braking mode and the bumping mode because of the dynamic effect.

In order to evaluate the effect of dynamic loading on the strains of pipes, the impact factor of strain is introduced as follows.

$$\eta = m / m_0 \qquad (1)$$

where m is the maximum strain in the pipes obtained from the dynamic loading, and m_0 is the static strain obtained from the same strain gauge, when the truck is placed along the same line. The impact factor of strain is computed for the front wheel, because its effect is sufficiently separated from the other two wheels, so that the values of m and m_0 can easily be evaluated.

4.1 Rolling Model

In Fig.8, the impact factor of strain obtained from the rolling tests with various rolling speed are plotted. The result for the cross sections A and E is shown, where A-1 and E-1 indicate the bottom of pipe and A-5 and E-5 indicate the crown of pipe. The same kind of symbol represents the same rolling corresponding to each speed. No significant difference is observed between the strain of the crown and that of the bottom. It implies that bending is also dominant for dynamic loading. The maximum impact factor of strain is observed at the speed of 15 km/h instead of the maximum speed of 30 km/h. They are η=1.1 and η=1.5 for the pipeline I and pipeline II, respectively. This phenomena seems relevant to the resonance of the truck.

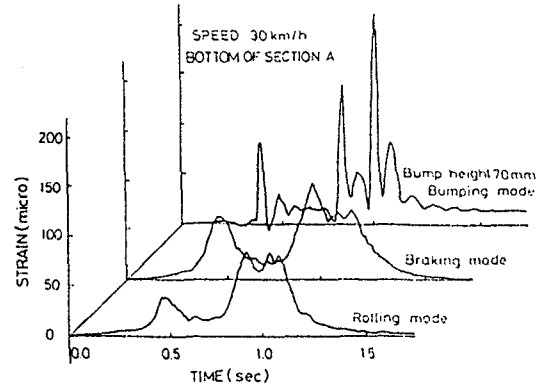

Fig.7 Profiles of strain caused by dynamic loading

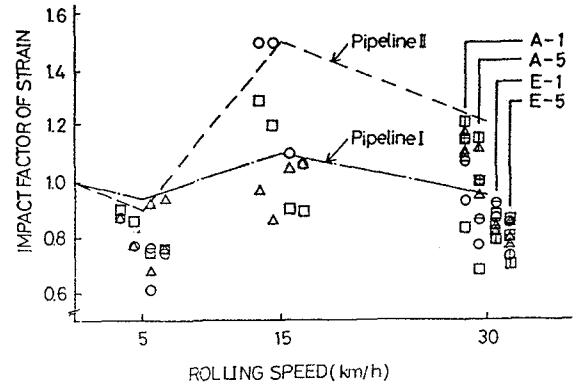

Fig.8 Profiles of strain caused by dynamic loading

4.2 Braking Mode

Fig.9 shows the comparison of the impact factor of strain between the rolling mode and the braking mode with different weight of the front wheel. As expected, the impact factor of strain from the braking mode is larger than that from the rolling mode and the weight of the front wheel affects the impact factor of strain. The maximum impact

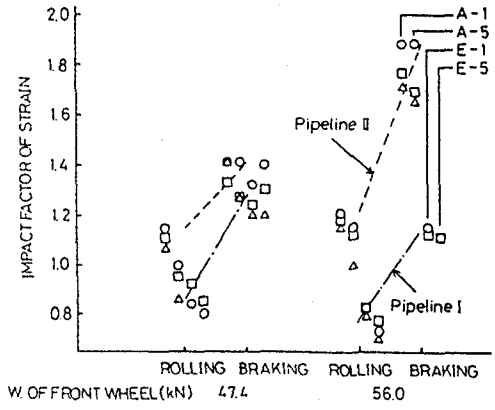

Fig.9 Impact factor of strain for rolling and braking mode

factors of 1.2 and 1.9 are obtained due to the wheel weight of 56 kN for the pipeline I and pipeline II, respectively.

4.3 Bumping Mode

Fig.10 shows the impact factor of strain with various bump heights for bumping mode, where the data from rolling mode is used for the bump height of h=0 cm or no bump. The impact factor of strain increases with the increase of the bump height, and the maximum values of 1.7 and 3.1 are obtained for the pipeline I and pipeline II, respectively.

In all the three modes of dynamic loading, the pipeline II, in which the pipeline is set perpendicular to the moving direction of trucks showed larger impact factor of strain.

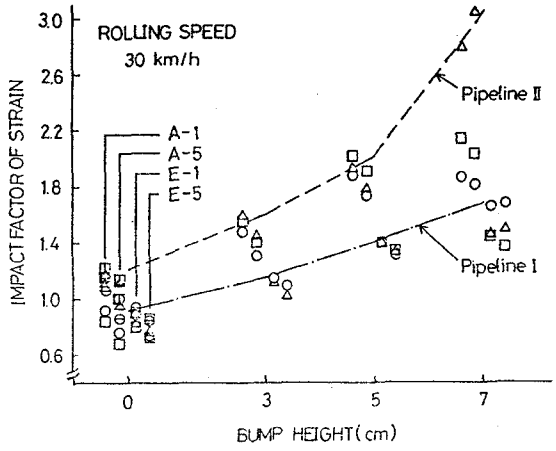

Fig.10 Impact factor of strain for different bump height

5. Parametric Analysis on Static Strain

5.1 Basic Conditions

Since the site conditions of the WSP are not always the same, it is necessary to determine the critical factors that affect the strain of pipes. Here, four factors, i.e. the installation depth, the reaction coefficient of bedding, the length of local hard bedding and the length of local soft bedding are included, and the analytical method described above is used to investigate the influence of each factor on the strains in a small diameter cast iron WSP. Among them, the local hard bedding (hereafter, LHB) simulates the rock inclusions or the crossing of other pipes beneath the pipes. The local soft bedding (hereafter, LSB) may exist where there is leakage of water from the pipes and the soil beneath the pipes become soft or is washed away.

Fig.11 shows the pipeline and the loading patterns used for the analysis. The pipeline consists of six cast iron pipes connected with socket joints. The diameter and length of each pipe are 100 mm and 4.0 m, respectively. The socket joint is typical for the connection of cast iron pipes. This type of joints can be assumed to be a rigid connection in the analysis. A truck with the same size as in the test is used as the loading truck. The weight of the truck is 196 kN (39.2 kN, 78.4 kN, 78.4 kN for the front axle, the front-rear axle and the rear-rear axle, respectively), which is comparable to the design truck specified in the Japanese Design Specification for the Highway Bridges. It is called loading pattern 1 when the truck is advanced along the pipeline, and loading pattern 2 when the truck is advanced across the pipeline.

The computed strains are normalized by the strain of 23 micro, which is the smaller value between the maximum strain of pipes under the two loading patterns when the installation depth is 1.2 m and the reaction coefficient of bedding is 9.8 N/cm^3, or a very weak bedding.

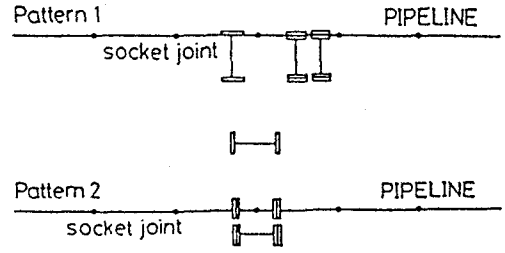

Fig.11 Loading patterns

5.2 The Influence of Reaction Coefficient and Depth

The specified installation depth of the WSP was changed several times in Japan. For example, for the pipes of 75 to 150 mm diameter, it was 0.8 m between 1950 and 1955, 1.0 m between 1956 and 1959, and 1.2 m since then. On the other hand, the reaction coefficient of bedding represents the rigidity of the bedding, which is usually the natural soil in the bottom of the trench. The reaction coefficient is correlated to the type and hardness of soil. For example, it varies from 7.8 to 83.3 N/cm^3 for saturated soil and from 2.2 to 88.2 N/cm^3 for clay. Based on these facts, the range of installation depth is considered as from 0.6 to 1.4 m and that of reaction coefficient of bedding as from 9.8 to 68.6 N/cm^3.

The normalized strain corresponding to various installation depth and reaction coefficient of bedding is shown in Fig.12. The strain increases with the decrease of both the depth and the reaction coefficient. The strain shows

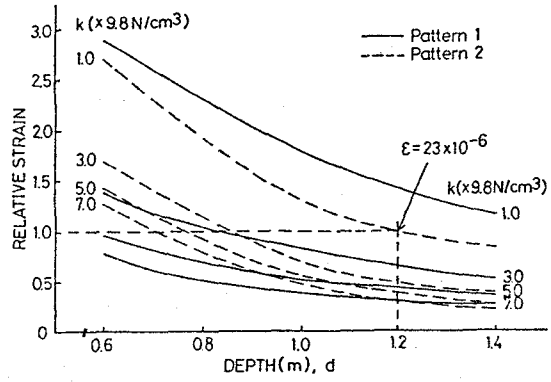

Fig.12 Relative maximum strain in pipeline with different depth and reaction coefficient

a rapid increase when the depth is less than 1.0 m and the reaction coefficient is less than 29.4 N/cm^3. The maximum strain is 67 micro and 62 micro for the pattern 1 and the pattern 2, respectively.

5.3 The Influence of Non-uniform Bedding

To clarify the influence of LHB and LSB, the truck is placed as shown in Fig.13 so as to obtain the maximum value of the strain. In the case of LHB, two heavy wheels or two double-tires are placed to bend the pipe, and in the case of LSB, the heaviest double-tire is placed right over the center of the LSB.

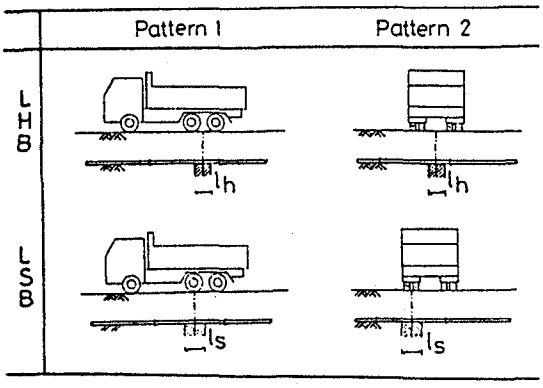

Fig.13 Loading location relative to the local hard bedding and local soft bedding

Fig.14 shows the analytical result corresponding to the extreme values of the depth and the reaction coefficient for the bedding with LHB. In the analysis, the value of the reaction coefficient of LHB is assumed to be 4.9 kN/cm^3, about 500 times larger than that of the surrounding soil. The strain increases with the decrease of the length of LHB. The pattern 2 shows much larger strain than the pattern 1 when both the depth and the reaction coefficient are small. When the length of LHB is 0.2 m, the maximum strains are obtained. They are 170 micro and 120 micro for the pattern 2 and the pattern 1, respectively.

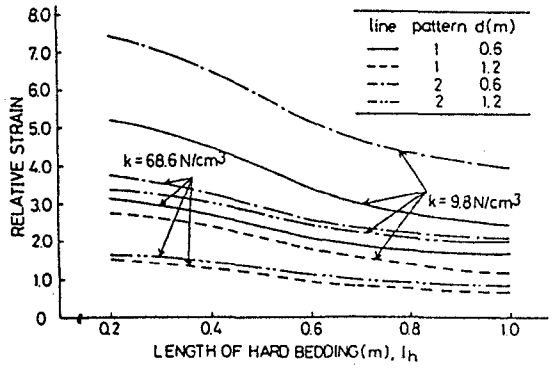

Fig.14 Effect of length of local hard bedding on maximum strain in pipeline

In the analysis for LSB, it is assumed that the reaction coefficient of LSB is 0.2 N/cm^3, which is negligibly small compared to that of surrounding soil. The length of LSB varies from 0 to 3.0 m. The strain increases rapidly with the increase of the length of LSB. The difference in the strain between the pattern 1 and the pattern 2 is negligibly small, as shown in Fig.15. When the length of LSB is 3.0 m, the maximum strain becomes 315 micro and 323 micro for the pattern 1 and the pattern 2, respectively. From the above analysis, it is clear that LHB and LSB are the most critical factors that affect the strain in the pipes, and that the load pattern 2 is the critical loading pattern in both LHB and LSB.

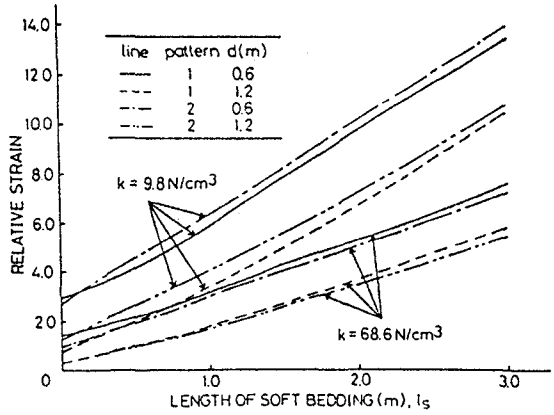

Fig.15 Effect of length of local soft bedding on maximum strain in pipeline

6. Computation of starin for durability evaluation

Concerning to durability, small diameter cast iron pipes is susceptible to two limit states, i.e. static limit state and fatigue limit state, in which static failure and fatigue failure are to be considered[9]. It is necessary to obtain the nominal strain of pipes for both limit states to evaluate the durability. We propose the following equation to compute the nominal strain in the pipes.

$$\varepsilon = \beta\varepsilon_o + \varepsilon_i \qquad (2)$$

where ε_i is the maximum basic strain of the pipes due to pipe installation and temperature change, ε_o is the maximum static strain caused by the wheel load of trucks and β is the maximum impact factor of strain.

The maximum basic strain ε_i can be computed using the following equation, in which it is assumed that the thermal expansion coefficient of cast iron is 1.0×10^{-5} and that the maximum strain caused by installation is 100 micro.

$$\varepsilon_i = (100 + 10 \cdot \Delta t_{max}) \times 10^{-6} \qquad (3)$$

where Δt_{max} represents the maximum temperature change.

The maximum static strain ε_o due to wheel load can be obtained using the same analytical method as that used in the parametric analysis. It is necessary to determine the truck load and the existence of LHB and LSB. The design truck load specified in the highway bridge design can be used in this analysis. The LHB is considered if the pipes are backfilled using original soil or when another pipeline or a concrete culvert lays beneath the pipe. The minimum length of the LHF of the site should be used in the analysis. The LSB is considered when water leakage may possibly occur in the pipeline, and the length of LSB is taken as 3.0 m. This value is given by considering that the leakage may wet the soil bedding along the pipe and the wet length expand until the leakage is discovered from the ground surface.

For the maximum impact factor of strain, β, the present test result obtained in the field test is used, although it may changes with site conditions, such as the installation depth, reaction coefficient of bedding, etc. It is because to obtain an analytical result or to carry out field test in every case is not always possible. The impact factor can be assumed as β =2.0 to cover the influence of rolling mode and braking mode. Depending to the surface condition of the road, the value is adopted corresponding to the bump height. Then β is taken as the maximum value of impact factors of strain from all dynamic tests.

6.1 Example Computation of the Maximum Strain in Pipes

The parameter of a cast iron pipeline of 100 mm diameter with socket joints are as follows; depth: 1.2 m, wall thickness: 7.5 mm, the reaction coefficient of bedding: 9.8 N/cm^3, length of LHB: 0.2 m, length of LSB: 3.0 m, road condition : relatively rough, maximum weight of truck: 196 kN, temperature change: 10 degree, loading pattern: 2.

1) to compute ε_i

According to Eq.2, we have

$$\varepsilon_i = (100 + 10 \times 10) \times 10^{-6} = 200 \times 10^{-6}$$

2) to obtain ε_o

By carrying out analysis for the loading pattern 1, we obtain $\varepsilon_o = 72 \times 10^{-6}$ for the LHB and $\varepsilon_o = 177 \times 10^{-6}$ for the LSB. Hence, we take $\varepsilon_o = 177 \times 10^{-6}$.

3) to obtain β

Since the road surface is rough, we adopt the bump height as 3 cm. Thus we have η=1.5 corresponding to the bumping mode. This value is taken as the value of β.

4) to compute ε

According to Eq.2, we obtain

$$\varepsilon = (1.5 \times 177 + 200) \times 10^{-6} = 465 \times 10^{-6}$$

7. Conclusion

This study aims at obtaining the longitudinal strains occurred in small diameter water supply pipes for durability evaluation. Field tests are carried out to investigate the strains of pipes under static load and dynamic load by using a dump truck. Then an analysis is carried out to compute the static strain of the pipelines, and the result is compared withthe experimental result. Parametric analysis is also carried out to investigate the critical factors that affect the static strain of pipes. Finally, an equation is proposed based on the computed static strain and the test results to obtain the nominal strain of small diameter water supply pipes for the durability evaluation.

The followings summarize the main findings.

1. The longitudinal strain in a small diameter pipeline under static loading can be evaluated by using the theory of beams on elastic foundation.
2. The static strain is amplified when the truck load is placed dynamically. The impact factor of strain attains to 1.5 in the rolling mode, 1.9 in the braking mode, and 1.5 to 3.1 in the bumping mode depending on the bump height.
3. The static strain shows a rapid increase when the depth and reaction coefficient of bedding are less than 1.0 m and 29.4 N/cm^3, respectively, or when there exist local hard bedding and local soft bedding. The latter is the most critical case for the static strain of pipes.

Acknowlegment

We are grateful to Assoc. Prof. H. Matsuzawa in the Department of Civil Engineering, Nagoya University, for his valuable advise, Mr. T. Okada and the members of South Office of Nagoya City Waterworks Bureau for their cooperation in the field tests.

References

1) Ma Zhiliang and Kentaro Yamada, Durability analysis of small diameter cast iron water supply pipes through sam -pling investigation, Journal of Structural Engineering, Vol. 40A, March 1994, pp.1129-1138. (In Japanese)
2) Nagoya City Waterworks Bureau and Department of Civil Engineering of Nagoya University, Research report on the evaluation of water supply pipes, pp.23-29, 1990. (In Japanese)
3) JIS G 5522, 1954. (In Japanese)
4) JIS G 5523, 1954. (In Japanese)
5) Japanese Waterworks Association, Specification and explanation for the design of waterworks facilities, pp.325 -334, pp.335-337, 1977. (In Japanese)
6) Pocock, R.G. et al., Behavior of shallow buried pipeline under static and rolling wheel load, Transport and Road Research Laboratory Report 954, 1980.
7) N. Takagi et al., An experiment on the longitudinal defo-rmation in small diameter buried pipelines subjected to vehicle loads, Tokyo Gas Technical Report No.31, 1987. (In Japanese)
8) N. Takagi et al., A method for analyzing longitudinal defo -rmation of buried pipes due to vehicle loads and its appli -cations, Tokyo Gas Technical Report No.29, 1985. (In Japanese)
9) Ma Zhiliang: Durability evaluaion of water supply pipes for establishing the replacement criterion, Doctoral Dissert -ation of Nagoya University, March. 1992. (In Japanese)

(Received September 14, 1994)